Am. J. Hum. Genet. 66:557–566, 2000

Evidence for Heterogeneity in Recombination in the Human Pseudoautosomal Region: High Resolution Analysis by Sperm Typing and Radiation-Hybrid Mapping

Sigbjørn Lien,[1,4] Joanna Szyda,[2] Birgit Schechinger,[3] Gudrun Rappold,[3] and Norm Arnheim[4]

[1]Department of Animal Science, Agricultural University of Norway, Aas, Norway; [2]Department of Genetics, Wroclaw Agricultural University, Wroclaw, Poland; [3]Institute of Human Genetics, Karl-Ruprecht University of Heidelberg, Heidelberg, Germany; and [4]Molecular Biology Program, University of Southern California, Los Angeles

Summary

Accurate genetic and physical maps for the human pseudoautosomal region were constructed by use of sperm typing and high-resolution radiation-hybrid mapping. PCR analysis of 1,912 sperm was done with a manual, single-sperm isolation method. Data on four donors show highly significant linkage heterogeneity among individuals. The most significant difference was observed in a marker interval located in the middle of the Xp/Yp pseudoautosomal region, where one donor showed a particularly high recombination fraction. Longitudinal models were fitted to the data to test whether linkage heterogeneity among donors was significant for multiple intervals across the region. The results indicated that increased recombination in particular individuals and regions is compensated for by reduced recombination in neighboring intervals. To investigate correspondence between physical and genetic distances within the region, we constructed a high-resolution radiation-hybrid map containing 29 markers. The recombination fraction per unit of physical distance varies between regions ranging from 13- to 70-fold greater than the genome-average rate.

Introduction

Human sex chromosomes recombine in the pseudoautosomal regions (PARs) located at the tips of the short and long arms of the X and Y chromosomes. A 50% recombination fraction in the Xp/Yp PAR (PAR1) suggested an obligatory crossover between the X and Y chromosomes during male meiosis (Burgoyne et al. 1982; Rouyer et al. 1986; Page et al. 1987). Absence of double recombinants in earlier studies suggested that only one recombination could occur in the human PAR1 (Rouyer et al. 1986), but later studies have reported a few double recombinants in the region (Rappold et al. 1994; Schmitt et al. 1994). The physical length of PAR1 is estimated to be 2.6 Mb by pulse field gel electrophoresis (PFGE) (Brown 1988; Petit et al. 1988; Rappold and Lehrach 1988). Efforts have also been made to cover PAR1 by yeast artificial chromosome (YAC) contigs (Slim et al. 1993*a*; Ried et al. 1995), but, owing to YAC instability, gaps may remain in the middle part of the region (Ried et al. 1995).

Although recombination plays a central role in genetics, much remains to be learned about its rate, pattern, and regulation in higher eukaryotes (Brooks 1988). Haldane (1922) was the first to suggest that some regions in the genome undergo recombination more frequently in the germ cells of one sex than the other. Since then, sex-specific differences in recombination have been well characterized in many organisms, including humans and mice (Donis-Keller et al. 1987; Roderick and Hillyard 1990; Broman et al. 1998), and recombination fractions are sometimes modeled separately for males and females. Likewise, within-sex variation of recombination has been proposed on the basis of bivalent chiasma frequencies observed in cytogenetic studies (Laurie and Hulten 1985). Recently, Broman et al. (1998) analyzed maternal haplotypes among the children of eight CEPH family mothers and showed that the total number of recombination events per gamete varied. Similar analysis of eight paternal haplotypes showed no differences. Data from several mammalian species show that recombination fractions per unit of physical distance vary between and along chromosomes. For example, telomeric regions are usually more recombinogenic than the rest of the chromosome (Donis-Keller et al. 1987; Nachman and Churchill 1996; Broman et al. 1998; Mohrenweiser et al. 1998). Hot spots of recombination (reviewed in Lichten and Goldman 1995; Robinson 1996) have been well

Received April 28, 1999; accepted for publication September 28, 1999; electronically published January 27, 2000.

Address for correspondence and reprints: Norman Arnheim, University of Southern California, 835 West 37th Street, Los Angeles, CA 90089-1340. E-mail: arnheim@molbio.usc.edu

0002-9297/2000/6602-0024$02.00

characterized in some species, but only limited information is available in mice (see Reeves et al. 1990; Bryda et al. 1992; Shirioshi et al. 1995), and very little is known about them in humans. Obviously, our understanding of recombination patterns in molecular terms will require very-high-resolution data, both at the physical and genetic levels, so that these patterns can eventually be defined in terms of DNA sequence and chromatin structure. Considering the growing databases of physical-mapping information in humans, the availability of accurate high-resolution recombination data is the limiting factor for comparison of physical and genetic information. The current maps provide an estimate of the recombination fraction averaged across all families studied, but chromosome regions that exhibit unusual recombination properties only in some individuals may not be identified.

Because of an almost unlimited number of sperm or meioses available from any male, sperm typing (Li et al. 1988) offers an opportunity to study recombination in single individuals. Recent sperm-typing experiments have shown evidence for individual variation in recombination in the chromosome region containing the major histocompatibility complex (MHC) of humans (Yu et al. 1996) and cattle (Park et al. 1995; Simianer et al. 1997), and the bovine PAR (Simianer et al. 1997). In regions with accurate physical maps, sperm typing also has the potential to dissect mammalian recombination hot spots to the point where DNA sequence analysis may reveal the molecular basis of hyperrecombination (Hubert et al. 1994). Recently, evidence for recombination heterogeneity adjacent to minisatellite sequences has been observed among individuals (Jeffrey et al. 1998).

In this study, we have applied sperm typing to test for individual variation of the recombination fraction in the human PAR. Furthermore, the construction of a high-resolution radiation hybrid (RH) map for PAR1 allowed the correspondence between physical and genetic distances within the region to be investigated.

Material and Methods

Donors and Markers

Among 43 donors genotyped for pseudoautosomal markers, 4 individuals with the greatest levels of heterozygosity for markers in the PAR were selected for single-sperm typing. The 4 individuals, all white, age 42–48 years, were heterozygous for a polymorphism (TEL) adjacent to the Xp/Yp telomere (Baird et al. 1995). Two sperm samples were analyzed for one of the donors at ages 47 and 48 years. Altogether, 1,912 single sperm were studied, and the number of sperm per donor had a range of 435–547.

Ten markers in PAR1, one marker in PAR2 (Xq/Yq), and five sex-specific loci were included in the study (table 1). The markers covered PAR1 almost completely, because one of the polymorphisms (TEL) is located only 652 bp from the Xp/Yp telomere repeat array (Baird et al. 1995).

Sperm Typing

Sorting and lysis of single sperm cells followed the method described by Lien et al. (1993) with minor modifications. The low-melting-point agarose containing the sperm was dried for 20 min at 37°C or until the agarose took on a "sticky" quality. Pieces of agarose, each containing a single sperm, were picked by using a thin scalpel blade close to the border where the agarose had not completely dried out. Agarose pieces were picked up by the tip on the side of the blade and transferred to 200-μl PCR tubes containing lysis buffer. DNA from single sperm was amplified by two rounds of PCR. The first was done with primer pairs for 16 loci. The final reaction contained: 5.0 μl lysis buffer (200 m*M* KOH, 50 m*M* DTT), 5.0 μl neutralization buffer (900 m*M* Tris-HCl, pH 8.3, 300 m*M* KCl, 200 m*M* HCl), 5.0 μl 10 × PCR buffer (100 m*M* Tris-HCl, pH = 8.3, 25 m*M* MgCl, 0.01% [weight/volume] gelatin), 0.15 m*M* each dNTP, 2.0 pmol each primer (table 1), 0.5 U *Taq* polymerase, and H_2O in a total volume of 50 μl. The PCR protocol was initiated with 3 min at 94°C, 2 min at 55°C, and 1 min at 72°C for cycle 1, followed by 15 s at 95°C, 1 min at 55°C, and 1 min at 72°C for cycles 2–5, and 15 s at 95°C, 30 s at 55°C, 30 s at 72°C for the last 35 cycles.

The products from the first round of PCR were reamplified in 16 separate locus-specific PCR reactions. The reactions were done in 10 mM Tris-HCl, pH 8.3, 50 mM KCl, 2.5 mM MgCl, and 0.001% (weight/volume) gelatin, with the addition of 0.2 mM of each dNTP, 10.0 pmol of each primer, 0.5 U *Taq* polymerase, 1.5 μl product from the first round of PCR, and H_2O in a total volume of 25 μl. The PCR protocol included 3 min at 94°C, followed by 15 s at 95°C, 30 s at 58°C, or 62°C, and 30 min at 72°C for 35 cycles. Primers and annealing temperatures for specific loci are given in table 1.

Scoring of alleles for TEL and DXYS15 and ZFX/ZFY was as previously described (Chong et al. 1993; Schmitt et al. 1994; Baird et al. 1995). Other markers in the study were di- or tetra-nucleotide repeats with an allele-length difference of $\geq$4 bp in the four selected donors. Genotypes were determined by electrophoresis in 3%–4% agarose gels and ethidium-bromide (EtBr) staining.

Multipoint Linkage Analysis

Marker order was established by multipoint linkage analysis by using a sperm-typing version of the MEN-

Table 1

Oligonucleotide Primers

Locus	Sequence (5′→3′)	PCR 1	PCR 2[a]
TEL (Baird et al. 1995)	AGGGACCGGGACAAATAGAC	+	
	CCAGACACACTAGGACCCTGAG	+	$+^{58}$
	TTGAAGTCCCCCCTGTGTAG		$+^{58}$
DXYS201 (Rappold et al. 1994)	ACGGACACAGAAATCCTTC	+	$+^{58}$
	TGTGATCCAATTTGCTAACA	+	$+^{58}$
DXYS15 (Schmitt et al. 1994)	TATTTATGGAAATTGCCCCC	+	
	TAATACAAGCCAGACGAGCC	+	$+^{62}$
	CACACATCACTGGAAATAGACTG		$+^{62}$
DXYS233 (Dib et al. 1996)	TTGGGAATTCGAGGCTGGA	+	
	TTGATTTCCATCCTGGGGTT	+	
	TGGGAAGACCCCCATCTCTG		$+^{62}$
	TCACGGCTCACAGCAGACTC		$+^{62}$
DXYS218 (Murray et al. 1994)	TGTGTTTGGGTTTCCTCTGTC	+	
	AGCGAAACTCCGTCTCAAAATA	+	$+^{62}$
	AACTGAGGGGACCTGGAATG		$+^{62}$
GGAT3F08 (Murray et al. 1994)	TTTTCCAGAAGCTCAGATCC	+	$+^{58}$
	CTGGGCAATGGAGTGAGAC	+	
	TATCCATCCATCCATCAACC		$+^{58}$
DXYS234 (Dib et al. 1996)	CCTAGCCTGGGCAGCAAG	+	$+^{62}$
	CTGAGGCGGGTCCCACAT	+	
	TTCCTGTTCCCCATCTCCA		$+^{62}$
DXYS85 (Schmitt et al. 1994)	ACCACAGGGCCTATCGTG	+	
	TTTGCTGAGCACCTAGAAGG	+	$+^{58}$
	TAGGTCCTCTAGGTGCAGGA		$+^{58}$
DXYS228 (Dib et al. 1996)	CCGGTCCCAACTATTAGCAGT	+	$+^{62}$
	TTTACGTGGGAGCAATAGTTCA	+	
	GTAATTAACAAACCGAGCTGTTA		$+^{62}$
MIC2 (Schmitt et al. 1994)	CAAATGCAGCTGATAAAA	+	$+^{58}$
	AGAGCTTCCTGTTTCTCC	+	$+^{58}$
AFM319yg5 (Dib et al. 1996)	ACCTCGTGAAAGACCCAATC	+	
	ATCACTAACTTGAGAGGTCCTATGT	+	$+^{62}$
	ATCATCCTTGCTCCCTAGAAC		$+^{62}$
AFMa082zh1 (Dib et al. 1996)	TCTGGGTGGATTGTGGAATAA	+	
	GGTTGCTGCAAATGCCATTA	+	$+^{58}$
	GCCATCAATCAACAGGTTGGT		$+^{58}$
AMG (Schaaff et al. 1996)	CTTCCCAGTTTAAGCTCTGATG	+	
	CCTTGCTCATATTATACTTGAC	+	
	CTGAGGGAGGTTCCATGA		$+^{58}$
	TGAGAAAACCAGGGTTCC		$+^{58}$
STS (Schmitt et al. 1994)	GAGTGAAACTCACTCAGCAC	+	$+^{62}$
	CCTTAGGAACCAGGAGATAC	+	
	TGGGAGACTGTCCCGAAGGT		$+^{62}$
	ACCGTACTTGCATGAGAAGCTGTCCCAAAGGA		$+^{62}$
ZFX/ZFY (Chong et al. 1993)	ACCA/GCTGTACTGACTGTGATTACAC	+	
	GCACC/TTCTTTGGTATCC/TGAGAAAGT	+	
	AC/TAACCACCTGGAGAGCCACAAGCT		$+^{58}$
	TGCAGACCTATATTCA/GCAGTACTGGCA		$+^{58}$
DXYS154 (Schmitt et al. 1994)	GCTTCGGCCTCCCAAAGT	+	
	ATGAAATTATCTGTTTGCTGATGAC	+	$+^{62}$
	GGCCTGAATTCATTTATTATTCTAATAG		$+^{62}$

[a] $+^{58}$ and $+^{62}$ denote primer combinations with annealing temperatures at 58°C and 62°C, respectively.

DEL linkage-analysis program (Lazzeroni et al. 1994). This program calculates recombination fractions and corresponding standard errors for adjacent loci by use of all data from all individuals simultaneously. Support for a given order was expressed by computing $\log_{10}(L_A/L_B)$, where L_A = maximum likelihood of the best-supported order and L_B = maximum likelihood for a given locus order.

RH Mapping

The protocol for TNG RH panel screening was generally as described by the manufacturer (Research Ge-

netics). Data were analyzed by using the RHMAP statistical package for multipoint RH mapping (Lange et al. 1995). The RH map was constructed by using the left-endpoint retention probability model under the multilocus ordering option of the program.

Testing the Variability of Recombination Fractions in Single Intervals

The heterogeneity of individual recombination fractions was first assessed separately for each of four marker intervals located within the PAR and the interval AFM319yg5-DXYS154 bracketing the region between PAR1 and PAR2. The Morton test (Morton 1956) was applied to test the variability of recombination fractions among donors, as described by Simianer et al. (1997). In addition to *P* values on the basis of the χ^2 distribution, empirical *P* values were obtained by permuting sperm-recombination status (i.e., recombinant or nonrecombinant) across donors 2,000 times (Churchill and Doerge 1994).

Another approach for testing the variability of recombination fractions was based on fitting various logistic-regression models. A series of null hypotheses of the form: H_0, $(\beta_m - \beta_{m'}) = 0$, was assessed by comparing parameter estimates (β) from two logistic-regression models by using the Wald test: $W = (\beta_m - \beta_{m'})' V_m^{-1} (\beta_m - \beta_{m'})$, where V_m^{-1} is the inverse of the variance-covariance matrix of b, and subscripts m and m' refer, respectively, to a less- and a more-parsimonious model. The asymptotic distribution of the Wald test follows the χ^2 distribution with df equal to the rank of V_m. The parameterization of vector β applied in different models is summarized in table 2.

Testing the Variability of Recombination Fraction across the Chromosome

To test whether the individual heterogeneity of recombination can be attributed to the chromosome as a whole, data from multiple intervals were analyzed together, by fitting logistic-regression models to the data from five marker intervals simultaneously. For fitted models, parameterization of donor effects was the same as that shown in table 2, but, in addition to donor effects, interval effects were also included. An important feature of the model was the assumed correlation between intervals located in the same sperm cell, meaning that a recombination status in one interval depends on a recombination status in other intervals. This is a longitudinal model for correlated binary data. Parameters were estimated on the basis of the generalized estimating equations (GEE) approach (Liang and Zeger 1986), assuming unstructured (co)variance of interval recombination status, common to all donors.

Table 2

Parameterization of Logistic-Regression Models

Model Number	β'	Model Parameterization
1N	$(\beta_1\ \beta_2\ \beta_3\ \beta_4)$	Separate parameter for each donor
2N	$(\beta_{12}\ \beta_{12}\ \beta_3\ \beta_4)$	Common parameter for A and B
3N	$(\beta_{13}\ \beta_2\ \beta_{13}\ \beta_4)$	Common parameter for A and C
4N	$(\beta_{14}\ \beta_2\ \beta_3\ \beta_{14})$	Common parameter for A and D
5N	$(\beta_1\ \beta_{23}\ \beta_{23}\ \beta_4)$	Common parameter for B and C
6N	$(\beta_1\ \beta_{24}\ \beta_3\ \beta_{24})$	Common parameter for B and D
7N	$(\beta_1\ \beta_2\ \beta_{34}\ \beta_{34})$	Common parameter for C and D
8N	$(\beta_{124}\ \beta_{124}\ \beta_3\ \beta_{124})$	Common parameter for A, B, and D
9N	$(\beta\ \beta\ \beta\ \beta)$	Common parameter for all donors

Results

Genetic Map

A multipoint linkage map was constructed on the basis of the genotype of 1,912 single sperm cells. The complete data set is available (see Electronic-Database Information). This map—flanked by a polymorphism (TEL), located only 652 bp from the Xp/Yp telomere repeat array (Baird et al. 1995), and DXYS154, located within the Xq/Yq PAR (PAR2)—defines a total length of 56.0 cM. The most-likely order of markers with individual recombination fractions for the four donors is presented in figure 1. The odds against the second-most-likely order, in which the closely linked markers DXYS228 and MIC2 were reversed, was $10^{1.6561}:1 \approx 45:1$. Two markers, AFM319yg5 (DXYS230) and AFMa082zh1 (DXYS229), previously localized to PAR1 (Dib et al. 1996), were mapped to the sex-specific part of X/Y. This location is supported by RH results (this study) and YAC contigs covering region Xp22.3–Xp21.3 (Ferrero et al. 1995). The overall efficiency of locus amplification in the sperm-typing experiment is high and varies from .899 to .972 for the 16 loci. Estimates of the probability of having one or zero sperm in the tube were .962 and .037, respectively, whereas the probability of picking more than one sperm was on the order of 1×10^{-5}. The nonspecific contamination rate per locus and sperm cell was .0030.

Double Recombinants

The analysis of 1,912 single sperm detected only 21 double recombinants for a segment with 0.56 cM genetic length, reflecting strong genetic interference. The double-crossover intervals were distributed throughout PAR1 as would be expected from a random process. By using a Poisson distribution of crossovers in 11 short marker intervals, and assuming that the number of crossovers is equivalent to the number of recombination events, we calculated the probability for two crossing-over events

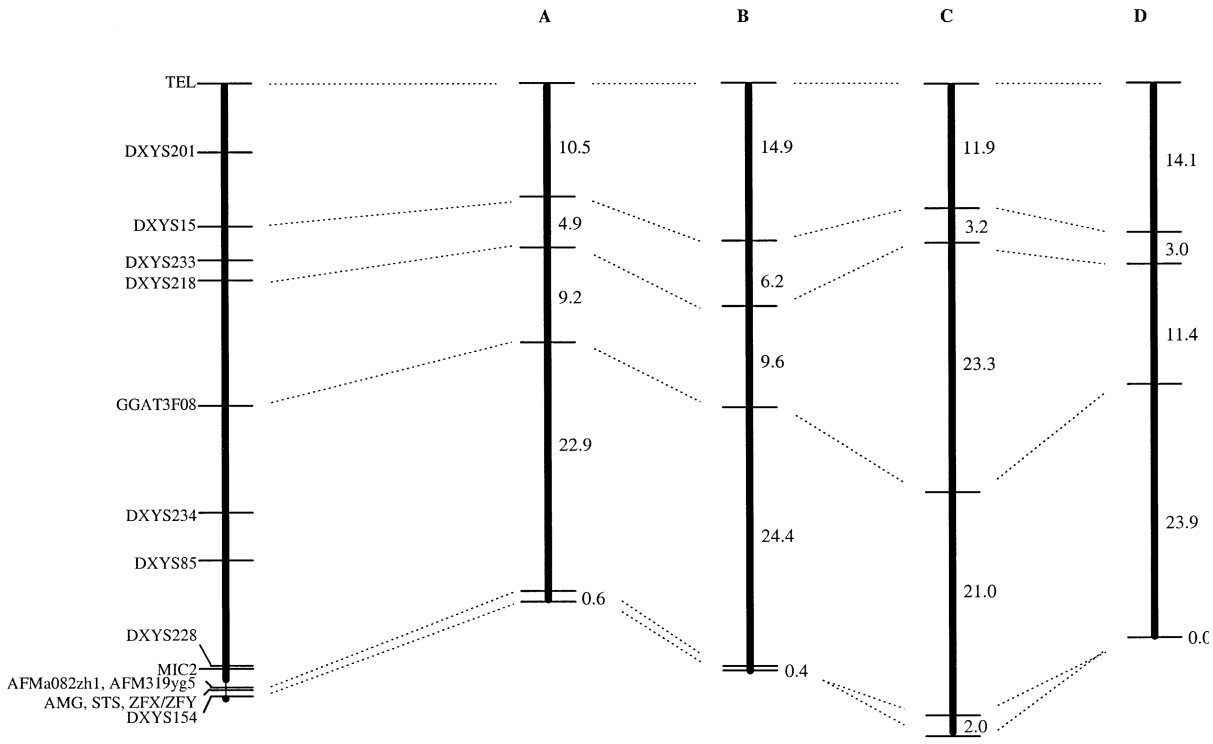

Figure 1 Male genetic map and individual recombination fractions (donors A–D) for five marker intervals on the human X/Y-chromosome.

to be .092331, or 177 among 1,912 sperm. Calculations made by using 2-point estimates of the recombination fractions from five larger intervals (fig. 1) yielded a similar probability: .076250, or 146 double-recombinant sperm. In 4 of the 21 double-crossover sperm cells, the two events were observed in neighboring intervals. When 11 marker intervals and the donor-average estimates of the recombination fractions are considered, the probability of recombination in any 2 neighboring intervals is .019245. Thus, among 1,912 sperm, we would expect ~37 (exactly 36.80) neighboring recombinants just by chance, which is more than eight times as many as the four observed events. All four were confirmed by retyping the first-round PCR product. Genotyping errors that produce single alleles in phase opposite to that of alleles from adjacent markers are suggested as the major source for false double recombinations in dense genetic maps (Buetow 1991; Broman et al. 1998). Analogously, contamination of the initial multiplex PCR reaction could account for these adjacent double crossovers. It is also possible that they result from a single recombination that was resolved to yield a gene-conversion event without flanking-marker exchange. The rest of the double recombinants were separated by at least two markers and are not likely to be the result of two independent genotyping errors.

Linkage Heterogeneity among Donors

Results from the Morton test (Morton 1956) for individual variability of recombination are presented in table 3. Two regions with significant linkage heterogeneity were detected. The most significant linkage heterogeneity among donors was observed for interval DXYS218–GGAT3F08 ($P < .00001$). Variability in the recombination fraction for single intervals was also tested by comparisons of logistic regression models with the Wald test (table 4). The results from this test are very similar to the results from the Morton test. The Wald test shows that linkage heterogeneity among donors in interval DXYS218–GGAT3F08 is caused by a more than two-fold increase in the recombination fraction in donor C, compared to the other individuals in the study. Fitting longitudinal models allows for simultaneous testing of linkage heterogeneity among donors in multiple intervals across the whole PAR1. This analysis produces no significant result (table 4), which indicates that donor C compensates for the higher recombination in interval DXYS218–GGAT3F08 with lower recombination elsewhere in the PAR1 (fig. 1).

Multiple sperm samples taken at two different ages were available for donor D. The comparison of recombination fractions at age 47 years (280 sperm) and age

Table 3

Morton Test for Linkage Heterogeneity among Donors at the X/Y Chromosome

Marker Interval	*n*	θ	*Z*	Pt	Pe
TEL-DXYS15	1618	.12361	224.22	.0662	.0745
DXYS15-DXYS218	1727	.04169	389.91	.0585	.0735
DXYS218-GGAT3F08	1721	.12435	237.42	<.00001	<.00001
GGAT3F08-AFM319yg5	1714	.23221	112.57	.3712	.3690
AFM319yg5-DXYS154	1710	.00760	481.59	.0037	.0040

NOTE.—Number of informative sperm (*n*), 2-point maximum-likelihood estimates of the recombination fraction (θ), with corresponding LOD score (*Z*), and type I–error probabilities for the Morton test on individual variability of the recombination fraction based on the χ^2 distribution (Pt) and permutation (Pe), for the five marker intervals on the X/Y chromosome.

48 years (267 sperm) for this donor revealed no significant differences for the 5-marker intervals shown in figure 1.

Physical Map

An RH map (table 5), including 29 markers from PAR1, was constructed by using the RHMAP statistical package for multipoint RH mapping (Lange et al. 1995). Proximal markers in the map are TEL located only 652 bp from to the Xp/Yp telomere repeat array (Baird et al. 1995) and DXYS77 (Schmitt et al. 1993) located ~14 kb from the PA boundary (Fisher et al. 1990). Another well-characterized locus located close to the PA boundary is *MIC2*. The gene is reported to be 52 kb in size (Smith et al. 1993) and maps 80 kb (Petit et al. 1988)–95 kb (Smith et al. 1993) from the PA-boundary and ~2,550 kb from Xptel (Petit et al. 1988). Comparing the distance of 2,550 kb with the RH map (707.7 cR), we obtain an average of 3.6 kb per 1% breakage for the human PAR1. This is similar to the genome average of 4 kb per 1% of X-ray breakage estimated for the TNG panel (Beasley et al. 1997). Five other markers included in the RH map have previously been mapped by PFGE (Petit et al. 1988; Rappold et al. 1992; Slim et al. 1993*b*). The physical distances per 1% of X-ray breakage for intervals containing these five markers vary from 3.2 kb, in interval DXYS17–MIC2, to 5.2 kb, in interval DXYS201–DXYS15.

Recombination per Unit of Physical Distance

On the basis of our data, recombination per unit of physical distance for the whole PAR1 is ~20-fold higher that the genome-average rate of 1 cM/Mb. The recombination fraction per unit of physical distance seems to be variable within different regions of the PAR1 (table 5). The most recombinant regions per unit of physical distance are (1) between DXYS201 and GGAT3F08, and (2) close to the PA-boundary, with a 26–38-fold increase in recombination compared to the genome average. Less recombination is observed in the region telomeric to DXYS201 and between markers GGAT3F04 and MIC2, with increases in recombination 13–23 times the genome-average rate.

Discussion

Linkage Heterogeneity among Donors

In humans, cytogenetic studies of bivalent chiasma frequencies have suggested individual variation among men in the position of crossovers (Laurie and Hulten 1985). Individual variation has also been inferred from limited human-family data supporting linkage heterogeneity on the basis of allele-specific effects on recombination between the markers Gm and alpha-1-antitrypsin (Gedde-Dahl et al. 1972; Weitkamp et al. 1978; Babron et al. 1990). Studies on the telomeric region of chromosome 4p have suggested that recombination may be suppressed in individuals carrying the HD mutation when compared to non-HD individuals (Buetow et al. 1991; MacDonald et al. 1989). Finally, sperm-typing analysis of recombination between the markers D6S291 and D6S109, which encompass the HLA region in single individuals, provided direct meiotic data on individual variation in the recombination fraction (Yu et al. 1996). A statistically significant difference was detected among five donors (range of recombination fractions 5.1%–11.2%). Our results on the human PAR1 also show linkage heterogeneity among donors. The most significant result was found for the interval DXYS218–GGAT3F08, where donor C has a more than two-fold increase in recombination fraction compared to the other individuals in the study ($P < .00001$). This variation could reflect polymorphisms in genes affecting recombination or differences in chromosome structure. Because the donors were of a comparable age, this variable can be excluded as contributory.

Table 4

Wald Test for Linkage Heterogeneity among Donors at the X/Y Chromosome

Marker Interval	Models							
	1N–9N	1N–2N	1N–3N	1N–4N	1N–5N	1N–6N	1N–7N	1N–8N
TEL-DXYS15	.0694	.3549	.1803	.9850	.9708	.5322	.2988	.3135
DXYS15-DXYS218	.0599	.9281	.1686	.2277	.4361	.5612	.9917	.2252
DXYS218-GGAT3F08	<.00001	≅1.0000	.0004	.8337	.0002	.8363	.0039	.7516
GGAT3F08-AFM319yg5	.3822	.9969	.5748	.9983	.6887	.9805	.4418	.9805
Multiple intervals[a]	.8996	.9559	≅1.0000	.9999	.9509	.9911	≅1.0000	.9409

Note.—Parameterization of donor effects 1 N–9 N are the same as in table 2. Type I error probabilities for the Wald test on individual variability of the recombination fraction are based on the χ^2 distribution.

[a] Simultaneously testing of intervals TEL-DXYS15, DXYS15-DXYS218, DXYS218-GGAT3F08, GGAT3F08-AFM319yg5, and AFM319yg5-DXYS1.

Pseudoautosomal Interference

Although linkage heterogeneity was detected in specific intervals, no significant heterogeneity among donors was detected when analyzing recombination throughout the XY pairing region (table 4). We conclude that donor C seems to compensate for the higher recombination in interval DXYS218–GGAT3F08 with a lower recombination in flanking intervals. This is in accordance with a strong positive linkage interference within the region and supports the old idea that the short physical distance reduces double recombination within human PAR1 during male meiosis (Rouyer et al. 1986). We detected ~1% double recombinants in the PAR1, in an interval of no more than 3 Mb. The fact that we detected so many double crossovers in PAR1 is in itself surprising. This raises the question of how the mechanism of interference works on both the scale of whole chromosomes (~50–250 Mb), where crossovers are restricted to between one and three, and in the ~2.6-Mb PAR1 (see Collins et al. 1996; Broman et al. 1998).

Physical Map of the PAR

Several YAC contigs that span the PAR have been characterized (Slim et al. 1993*a*; Ried et al. 1995). Despite intensive efforts to cover the whole PAR1, high levels of YAC instability have made this work very difficult, and gaps may remain in the middle part of the region (Ried et al. 1995). An alternative physical-mapping strategy to YACs is RH mapping facilitated by the development of a high-resolution (TNG) mapping panel (Beasley et al. 1997). Our high resolution RH map for PAR1 (table 5), fits very well with previously published cosmid contigs covering the first 700 kb of Xptel (Rao et al. 1997) and with PFGE results on the whole region (Petit et al. 1988; Rappold et al. 1992; Schiebel et al. 1993). However, discrepancies in locus order are found when comparing the RH map with YAC contigs for the middle part of PAR1. On the basis of the RH mapping, the location of markers DXYS141, DXYS234, and DXYS138 are between ANT3 and DXYS85. This is in conflict with YAC contigs generated for the region (Slim et al. 1993*a*; Ried et al. 1995) but agrees with linkage data in this study. Also the positions of DXYS85 and DXYS17 in the RH map are different from previous reports (Slim et al. 1993*a*; Ried et al. 1995). Recently, Ried et al. (1998) showed that, as a result of gene duplications, some DNA sequences exist at both 800–1000 kb and 1800–2100 kb from the Xptel. This may at least partly explain discrepancies in results obtained by different physical-mapping methods.

Comparison between the Physical and Genetic Maps

Currently available genetic maps, although dense in markers, are relatively low in resolution; the individual genetic distances between closely linked markers have wide confidence intervals. The construction of a high-resolution genetic map and an overlapping RH map allows us to make a more accurate comparison between physical and genetic distances in PAR1. A 50% recombination fraction within 2.6 Mb of the human PAR1 implies recombination per unit of physical distance at ~20 times the genome average. The sperm-typing results in this study confirm this highly elevated recombination fraction for the whole PAR1 but show that recombination per unit of physical distance varies considerably within the region (table 5). The highest recombination fraction per Mb is found for interval DXYS201–GGAT3F04 and the interval adjacent to the PA-boundary (table 5). Our results for this latter interval are consistent with the data of Schmitt et al. (1994), who estimated recombination in this region to be 31-fold higher than the genome average. Similarly, highly elevated recombination per unit of physical distance was detected between DXYS201 and GGAT3F08 located 468–1162 kb from the Xptel. This region contains the 331-kb marker interval DXYS218–GGAT3F08 where we also observe linkage heterogeneity among donors. Assuming no major rearrangements or duplications in the region,

Table 5

RH Map and Correspondence between Physical and Genetic Distances in the Human PAR1

	Physical Map			Genetic Map[d]	Recombination per Physical Unit	
Markers[a]	RH Map (cR)	~kb[b]	PFGE[c]	(cM)	cM/~kb[b]	Increase[e]
TEL	.0	0		0		
DXYS14	.7					
DXYS129	36.9				7.2/468	15-fold
DXYS60	58.8					
DXYS153	95.4					
DXYS201	117.0	468	450	7.2		
DXYS131	139.3					
DXYS136	163.1				6.3/231	27-fold
DXYS15	174.7	699	750	13.5		
DXYS233	183.5				4.2/132	32-fold
DXYS218	207.8	831		17.7		
DXYS137	222.8					
DXYS91	231.4				12.5/331	38-fold
GGAT3F08	290.4	1162		30.2		
CSF2RA	317.9	1272	1200–1300			
ANT3	340.3	1361	1300		9.8/435	23-fold
DXYS141	371.9					
DXYS234	399.2	1597		40.0		
DXYS138	406.4				4.3/253	17-fold
DXYS85	462.5	1850		44.3		
DXYS17	519.4	2077	1900–2000			
DXYS145	521.6					
DXYS147	587.4					
DXYS93	599.7					
DXYS152	653.9				9.7/754	13-fold
DXYS151	653.9					
DXYS228	707.7					
MIC2	707.7	2831	2550	54.0		
DXYS77	735.2				1.3/50	26-fold
PA-boundary		2881	2600	55.3		

[a] Markers used to define the genetic map intervals are shown in bold.

[b] Transformation of X-ray breakage to physical distance performed with the TNG panel (1% breakage = 3.6 Kb).

[c] Physical distance in kb, according to PFGE (Petit et al. 1988; Rappold et al. 1992; Slim et al. 1993*b*).

[d] Sperm-typing multipoint estimates of the recombination fraction, made with the Kosambi map function.

[e] Recombination per unit of physical distance, compared to the genome-average rate of 1 cM/1,000 kb.

donor C has a recombination fraction 70-fold higher than the genome average in this interval. The development of additional markers in this region could allow identification of the hyperrecombinogenic interval at a higher resolution.

Sperm-Typing Methodology

Finally, single sperm cells were obtained by suspending the sperm in low-melting-point agarose and picking sperm manually under an inverted phase microscope (Lien et al. 1993). The method has been shown to be highly accurate (Lien et al. 1993; Klungland et al. 1997; Simianer et al. 1997; Lien et al. 1999), as confirmed for human sperm in this study by a negligible frequency of more than one sperm per tube and a very low nonspecific contamination rate. As a consequence, recombination fractions estimated by a sperm-typing version of the MENDEL program were almost identical to estimates from 2-point linkage analysis without taking specific errors in the sperm-typing approach into account. Because of the cost of the equipment and the technical difficulties

of FACS sorting for single-sperm isolation, use of the agarose gel procedure should be considered for experiments involving moderate sample sizes.

Acknowledgments

We thank Charles Tilford for helpful discussions and for sharing unpublished physical-mapping information on the human PAR1. This work was supported in part by grant R37-GM36745 from the National Institutes of General Medical Sciences.

Electronic-Database Information

Accession numbers and URLs for data in this article are as follows:

http://www.usc.edu/dept/LAS/biosci/arnheim (for the complete sperm-typing data set)

References

Babron MC, Constans J, Dugoujon JM, Cambon-Thomsen A, Bonaiti-Pellie C (1990) The Gm-Pi linkage in 843 French families: effect of the alleles Pi Z and Pi S. Ann Hum Genet 54:107–113

Baird DM, Jeffreys AJ, Royle NJ (1995) Mechanisms underlying telomere repeat turnover, revealed by hypervariable variant repeat distribution patterns in the human Xp/Yp telomere. EMBO J 14:5433–5443

Beasley EM, Stewart EA, McKusick KB, Aggerwal A, Brady-Hebert S, Fang NY, Hadley D, et al (1997) TNG4 radiation hybrid maps improve the resolution of the G3 RH maps of the human genome. In: Genome mapping and sequencing 1997. Cold Spring Harbor Laboratory Press, Cold Spring Harbor, NY

Brooks LD (1988) The evolution of recombination rates. In: Michod RE, Levin BR (eds) The evolution of sex: an examination of current ideas. Sinauer, Sunderland, MA, pp 87–105

Broman KW, Murray JC, Sheffield VC, White RL, Weber JL (1998) Comprehensive human genetic maps: individual and sex-specific variation in recombination. Am J Hum Genet 63:861–869

Brown WR (1988) A physical map of the human pseudoautosomal region. EMBO J 7:2377–2385

Bryda EC, DePari JA, Sant'Angelo DB, Murphy DB, Passmore HC (1992) Multiple sites of crossing over within the Eb recombinational hotspot in the mouse. Mamm Genome 2: 123–129

Buetow KH, Shiang R, Yang P, Nakamura Y, Lathrop GM, White R, Wasmuth JJ, et al (1991) A detailed multipoint map of human chromosome 4 provides evidence for linkage heterogeneity and position-specific recombination rates. Am J Hum Genet 48:911–925

Burgoyne PS (1982) Genetic homology and crossing over in the X and Y chromosomes of mammals. Hum Genet 61: 85–90

Chong SS, Kristjansson K, Cota J, Handyside AH, Hughes MR (1993) Preimplantation prevention of X-linked disease: reliable and rapid sex determination of single human cells by restriction analysis of simultaneously amplified ZFX and ZFY sequences. Hum Mol Genet 2:1187–1191

Churchill GA, Doerge RW (1994) Empirical threshold values for quantitative trait mapping. Genetics 138:963–971

Collins A, Frezal J, Teague J, Morton NE (1996) A metric map of humans: 23,500 loci in 850 bands. Proc Natl Acad Sci USA 93:14771–14775

Dib C, Faure S, Fizames C, Samson D, Drouot N, Vignal A, Millasseau P, et al (1996) A comprehensive genetic map of the human genome based on 5,264 microsatellites. Nature 380:152–154

Donis-Keller H, Green P, Helms C, Cartinhour S, Weiffenbach B, Stephens K, Keith TP, et al (1987) A genetic linkage map of the human genome. Cell 51:319–337

Ferrero GB, Franco B, Roth EJ, Firulli BA, Borsani G, Delmas-Mata J, Weissenbach J, et al (1995) An integrated physical and genetic map of a 35 Mb region on chromosome Xp22.3-Xp21.3. Hum Mol Genet 4:1821–1827

Fisher EM, Alitalo T, Luoh SW, de la Chapelle A, Page DC (1990) Human sex-chromosome-specific repeats within a region of pseudoautosomal/Yq homology. Genomics 7:625–628

Gedde-Dahl T Jr, Fagerhol MK, Cook PJ, Noades J (1972) Autosomal linkage between the Gm and Pi loci in man. Ann Hum Genet 35:393–399

Haldane JBS (1922) Sex ratio and unisexual sterility in hybrid animals. J Genet 12:101–109

Hubert R, MacDonald M, Gusella J, Arnheim N (1994) High resolution localization of recombination hot spots using sperm typing. Nat Genet 7:420–424

Jeffreys AJ, Murray J, Neumann R (1998) High resolution mapping of crossovers in human sperm defines a minisatellite-associated recombination hotspot. Mol Cell 2:267–273

Klungland H, Gomez-Raya L, Howard CJ, Collins RA, Rogne S, Lien S (1997) Mapping of bovine FcgammaR (FCGR) genes by sperm typing allows extended use of human map information. Mamm Genome 8:573–577

Lange K, Boehnke M, Cox DR, Lunetta KL (1995) Statistical methods for polyploid radiation hybrid mapping. Genome Res 5:136–150

Laurie DA, Hulten MA (1985) Further studies on bivalent chiasma frequency in human males with normal karyotypes. Ann Hum Genet 49:189–201

Lazzeroni LC, Arnheim N, Schmitt K, Lange K (1994) Multipoint mapping calculations for sperm-typing data. Am J Hum Genet 55:431–436

Li HH, Gyllensten UB, Cui XF, Saiki RK, Erlich HA, Arnheim N (1988) Amplification and analysis of DNA sequences in single human sperm and diploid cells. Nature 335:414–417

Liang KY, Zeger S (1986) Longitudinal data analysis using generalized linear models. Biometrika 73:13–22

Lien S, Kaminski S, Alestrom P, Rogne S (1993) A simple and powerful method for linkage analysis by amplification of DNA from single sperm cells. Genomics 16:41–44

Lien S, Cockett NE, Klungland H, Arnheim N, Georges M,

Gomez-Raya L (1999) High-resolution gametic map of the sheep callipyge region: linkage heterogeneity among rams detected by sperm typing. Anim Genet 30:42–46

Lichten M, Goldman ASH (1995) Meiotic recombination hotspots. Annu Rev Genet 29:423–444

MacDonald ME, Haines JL, Zimmer M, Cheng SV, Youngman S, Whaley WL, Wexler N, et al (1989) Recombination events suggest potential sites for the Huntington's disease gene. Neuron 3:183–190

Mohrenweiser HW, Tsujimoto S, Gordon L, Olsen AS (1998) Regions of sex-specific hypo- and hyper-recombination identified through integration of 180 genetic markers into the metric physical map of human chromosome 19. Genomics 47:153–162

Morton NE (1956) The detection and estimation of linkage between genes for elliptocytosis and the Rh blood type. Am J Hum Genet 8:80–96

Murray JC, Buetow KH, Weber JL, Ludwigsen S, Scherpbier-Heddema T, Manion F, Quillen J (1994) A comprehensive human linkage map with centimorgan density. Cooperative Human Linkage Center (CHLC). Science 265:2049–2054

Nachman MW, Churchill GA (1996). Heterogeneity in rates of recombination across the mouse genome. Genetics 142: 537–548

Page DC, Bieker K, Brown LG, Hinton S, Leppert M, Lalouel JM, Lathrop M, et al (1987) Linkage, physical mapping, and DNA sequence analysis of pseudoautosomal loci on the human X and Y chromosomes. Genomics 1:243–256

Park C, Russ I, Da Y, Lewin, HA (1995) Genetic mapping of F13A to BTA23 by sperm typing: difference in recombination rate between bulls in the DYA-PRL interval. Genomics 27:113–118

Petit C, Levilliers J, Weissenbach J (1988) Physical mapping of the human pseudo-autosomal region; comparison with genetic linkage map. EMBO J 7:2369–2376

Rao E, Weiss B, Fukami M, Mertz A, Meder J, Ogata T, Heinrich U, et al (1997) FISH-deletion mapping defines a 270-kb short stature critical interval in the pseudoautosomal region PAR1 on human sex chromosomes. Hum Genet 100: 236–239

Rappold GA, Lehrach H (1988) A long range restriction map of the pseudoautosomal region by partial digest PFGE analysis from the telomere. Nucleic Acids Res 16:5361–5377

Rappold G, Willson TA, Henke A, Gough NM (1992) Arrangement and localization of the human GM-CSF receptor alpha chain gene CSF2RA within the X-Y pseudoautosomal region. Genomics 14:455–461

Rappold GA, Klink A, Weiss B, Fischer C (1994) Double crossover in the human Xp/Yp pseudoautosomal region and its bearing on interference. Hum Mol Genet 3:1337–1340

Reeves RH, Crowley MR, O'Hara BF, Gearhart JD (1990) Sex, strain, and species differences affect recombination across an evolutionarily conserved segment of mouse chromosome 16. Genomics 8:141–148

Ried K, Mertz A, Nagaraja R, Trusgnich M, Riley JH, Anand R, Lehrach H, et al (1995) Characterization of a YAC contig spanning the pseudoautosomal region. Genomics 10:787–792

Ried K, Rao E, Schiebel K, Rappold GA (1998) Gene duplications as a recurrent theme in the evolution of the human pseudoautosomal region 1: isolation of the gene ASMTL. Hum Mol Genet 7:1771–1778

Robinson WP (1996) The extent, mechanism and consequences of genetic variation, for recombination rate. Am J Hum Genet 59:1175–1183

Roderick TH, Hillyard AL (1990) Differences in recombination due to sex in mice. Mouse News Lett 85:87

Rouyer F, Simmler MC, Johnsson C, Vergnaud G, Cooke HJ, Weissenbach J (1986) A gradient of sex linkage in the pseudoautosomal region of the human sex chromosomes. Nature 319:291–295

Schaaff F, Wedemann H, Schwinger E (1996) Analysis of sex and delta F508 in single amniocytes using primer extension preamplification. Hum Genet 98:158–161

Schiebel K, Weiss B, Wohrle D, Rappold G (1993) A human pseudoautosomal gene, ADP/ATP translocase, escapes X-inactivation whereas a homologue on Xq is subject to X-inactivation. Nat Genet 3:82–87

Schmitt K, Vollrath D, Foote S, Fisher EM, Page DC, Arnheim N (1993) Four PCR-based polymorphisms in the pseudoautosomal region of the human X and Y chromosomes. Hum Mol Genet 2:1978

Schmitt K, Lazzeroni LC, Foote S, Vollrath D, Fisher EM, Goradia TM, Lange K, et al (1994) Multipoint linkage map of the human pseudoautosomal region, based on single-sperm typing: do double crossovers occur during male meiosis? Am J Hum Genet 55:423–430

Shiroishi T, Koide T, Yoshino M, Sagai T, Moriwaki K (1995) Hotspots of homologous recombination in mouse meiosis. Adv Biophys 31:119–132

Simianer H, Szyda J, Ramon G, Lien S (1997) Evidence for individual and between-family variability of the recombination rate in cattle. Mamm Genome 8:830–835

Slim R, Le Paslier D, Compain S, Levilliers J, Ougen P, Billault A, Donohue SJ (1993*a*) Construction of a yeast artificial chromosome contig spanning the pseudoautosomal region and isolation of 25 new sequence-tagged sites. Genomics 16: 691–697

Slim R, Levilliers J, Ludecke HJ, Claussen U, Nguyen VC, Gough NM, Horsthemke B (1993*b*) A human pseudoautosomal gene encodes the ANT3 ADP/ATP translocase and escapes X-inactivation. Genomics 16:26–33

Smith MJ, Goodfellow PJ, Goodfellow PN (1993) The genomic organization of the human pseudoautosomal gene MIC2 and the detection of a related locus. Hum Mol Genet 2:417–422

Weitkamp LR, Cox D, Guttormsen S, Johnston E, Hempfling S (1978) Allelic specific heterogeneity in the Pi:Gm linkage group. Cytogenet Cell Genet 22:647–650

Yu J, Lazzeroni L, Qin J, Huang MM, Navidi W, Erlich H, Arnheim N (1996) Individual variation in recombination among human males. Am J Hum Genet 59:1186–1192